

Some Features of Aerosols and Pre-cursor Gases Observed over Antarctic Region during 24th Indian Antarctic Expedition

P.C.S. Devara and S.M. Sonbawne

Indian Institute of Tropical Meteorology, Dr. Homi Bhabha Road, Pune 411 008
Tel. +91-020-25893600; Fax: +91-020-25893825; E-Mail: devara@tropmet.res.in

ABSTRACT

The aerosols and pre-cursor gases data sets have been utilized to investigate the aerosol optical, physical and radiative properties, and their interface with simultaneously measured gases. Data over the Oceanic region has been collected on ship's front deck. The daily mean AOD at a characteristic wavelength of 500 nm was found to be 0.042 with an average Angstrom coefficient of 0.24, revealing abundance of coarse-mode particles. Interestingly, the January fluxes were found to be less by about 20 per cent as compared to those in February. The average short-wave direct radiative forcing due to aerosols showed cooling at the surface with an average value of -0.47 W/m^2 during the study period. The total column ozone increased from about 252 DU around 38°S to about 312 DU at 70°S , showing a gradual increase in ozone with increasing latitude. The TCO measured by the surface-based ozone monitor matched reasonably well with that observed by the Total Ozone Mapping Spectrometer (TOMS) satellite sensor within 5%. Variability in ozone on daily scale, during the study period, was less than 4% over the Antarctica region. In this report, we briefly describe the equipment deployed, data archival and analysis techniques and some salient results obtained from the measurements made during the above period.

INTRODUCTION

Aerosols are a minor component of the atmosphere in free troposphere and aloft. They mostly form due to gas-to-particle conversion processes. Aerosols may be natural or anthropogenic in origin. The main mechanisms by which atmospheric aerosols are formed include break-up of materials and agglomeration of molecules. Once formed, aerosol may undergo different changes caused by physico-chemical reaction processes such as diffusion, coagulation, sedimentation, evaporation and nucleation.

Coagulation process controls the smaller particle end of the aerosol size distribution. The sedimentation process depends on both diffusion coefficient as well as fall velocity of particles. The study of aerosols is important for various reasons. For example, (i) aerosols influence the climate directly by altering the radiative energy transfer through their optical properties, and (ii) space-time variability of aerosol in homogeneities are needed for environmental research.

The importance of aerosols on climate forcing has been very well established (Penner et al., 2001; Ramanathan et al., 2001). Aerosols can change Earth's radiation budget both directly by scattering and absorbing radiation and indirectly by affecting cloud properties (Russell et al., 1999). Changing the net flux of radiation above or within the atmosphere alters the energy available for driving the Earth's climate. Hence such a net flux change is termed as radiative forcing of climate (IPCC, 1995). Particles in the atmosphere scatter the incoming solar radiation and thus reduce the radiation flux reaching the Earth (dimming). This is known as 'direct radiative effect' and it accounts for negative forcing. Negative forcing tends to cool the climate and positive forcing tend to warm it. Aerosol particles, particularly those with high black carbon (BC) content, are capable of absorbing incoming solar radiation. While this also decreases the radiation flux at the surface, it heats the atmosphere locally. This heating can, in turn, cause a third climate forcing effect known as the 'semi-direct radiative effect'; the heating of the atmosphere can suppress the local relative humidity (RH) and there by reduce the change of cloud formation.

The polar-regions play an important role in global change studies because enhanced warming is predicted for high-latitudes as greenhouse gas and aerosol concentrations continue to increase in the atmosphere. Global warming is believed to be primarily due to significant increase in the so-called greenhouse gases of which troposphere ozone is one important component. Aerosols and pre-cursor gas observations over Antarctic region play great role not only in the Earth's radiation budget but provide reference levels for all environmental and pollution studies due to its remoteness and restricted human activities. Thus, in this region, while the total mass of the aerosol particles suspended in the vertical atmospheric column of unit cross section yields smaller values, the lower aerosol optical depth at all the visible and near-infrared wavelengths is of great concern for Earth's radiation budget studies. The attenuation of solar irradiance and the processes of scattering and absorption by the aerosol particles may cause

appreciable effects on the radiative exchange mechanisms occurring in the Antarctic atmosphere. Hence the aerosol properties and their effects on weather and climate of this region are certainly different from other continental areas. Moreover, the study of heterogeneous chemistry of aerosols - an unique phenomenon of polar regions, provides information on gas-to-particle conversion processes leading to formation of secondary aerosol particles and their influence on ozone content. Studies have shown that the warming can be nearly 4-5 times more over the poles compared to that over tropics. Thus the atmosphere over Antarctica is very sensitive to human-induced changes in any part of the globe and dynamics of the atmosphere over Antarctica itself seems to modify global weather and climate. Two important problems or concerns of the present-day scientific community are the ozone hole and the aforementioned global greenhouse warming; the former already having manifested prominently over Antarctica during the past decade (WMO, 2003), and the latter having started showing indications of its effects at mid and polar latitudes. Thus there is a need to continuously keep monitoring of the atmospheric constituents over this sensitive region of Antarctica.

Ever since the establishment of Indian stations, Dakshin Gangotri in 1983-84 and Maitri in 1988-89 at Antarctica, Indian scientists have been very much involved in Antarctic research (Rajaram and Reddy, 1993). Several summer and winter expeditions have been undertaken since the beginning where atmospheric scientists have taken active part in monitoring and studying atmospheric constituents (Gadhavi and Jayaraman, 2003; Jain et al., 2004). Within the frame work of the 24th Indian Antarctica Expedition (IAE), we have carried out observations of total column aerosol optical depth (AOD), ozone (TCO) and precipitable water content (TCW) using a multi-channel solar-radiometer (Microtops II); and short-wave global radiative flux using a wide-band pyranometer over the Indian Antarctica station 'Maitri' (70.76° S, 11.74° E) and southern Indian Ocean during December 2004-February 2005.

EXPERIMENTAL SITE AND MEASUREMENT TECHNIQUES

The Indian Antarctica Station, "Maitri", is located in the Schrimacher Oasis in the Dronning Maud Land, East Antarctica (117 m MSL). The nearest steep cliff of the east west trending glacier on the southern side of the station is more than 700 m away from the station and is 300 m in height. The snow covered surface during summer season is more than 0.5 km away from the station. The instruments were installed on barren land near the

station. The surface of the station area is mainly covered by sandy and loamy sand types of soil (Panneerselvam, et. al., 2004). Antarctica has a desert like climate with clear skies, very low atmospheric aerosol content. During summer, the prevailing winds are light, following nearly constant direction, and are relatively free from turbulent and convective motions. The cloud cover over the station occurs mainly under the influence of sub polar low-pressure systems and shows an alternating sequence of clear sky changing over to the overcast and again clearing as the system moves away.

Hand-held Radiometer (MICROTOPS II)

This instrument consists of sun photometer and ozonometer. It measures the columnar AOD and Ozone, water vapor at selected wavelengths which in turn provide the attenuation in sunlight reaching the ground due to the presence of aerosol pollutants. **Figure 1** depicts the instrument. This radiometer provides integrated AOD (extinction) at six wavelengths covering from UV to NIR and ozonometer determines total column ozone (at UV wavelengths) and perceptible water content (at NIR band) simultaneously. The built-in solid state pressure sensor provides the

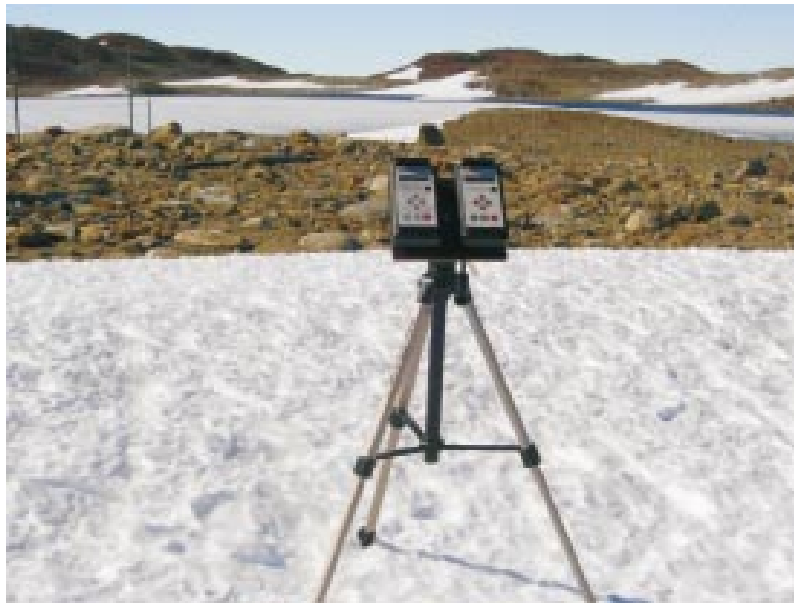


Fig. 1: Photograph of Microtops II (Sun photometer and Ozonometer) operating at Maitri

current atmospheric pressure needed for calculation of scattering due to air molecules (Rayleigh). The global positioning system GPS receiver provides the geographical coordinates of the site, which are used for estimating the local air mass.

When the instrument is switched on the radiation captured by its collimators pass through the band-pass filters and falls onto the photodiode. These signals are amplified and at the same time they store the background value for all the filters (sets of over 25 observations for each filter). The average value, obtained for each filter is used to compute the spectral variation of columnar AOD, ozone and water vapor instantaneously and display for quick look.

Short-wave Pyranometer

The pyranometer is an instrument used to measure direct and diffuse shortwave radiation arriving from the whole hemisphere (usually complete sky). **Figure 2** displays the basic sensor and data acquisition system of the

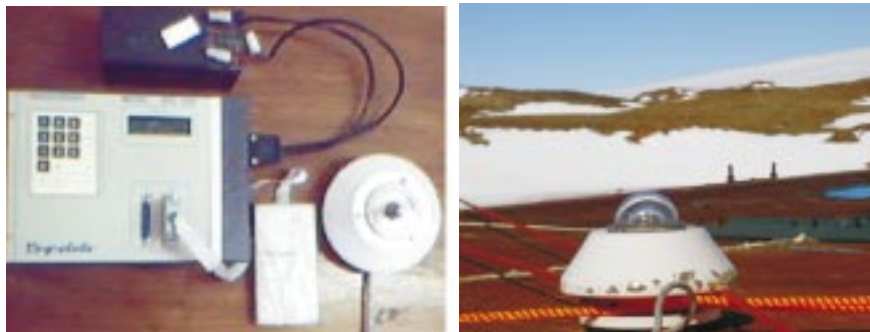


Fig. 2 : Photograph of the global short-wave pyranometer with data acquisition system. Location of the sensor in the Antarctic environment can also be seen in the figure

instrument. This instrument measures the total radiation with an unobstructive view. Some pyranometers can be inverted to measure the reflected shortwave radiation from a surface. The pyranometer used in the present study has a circular multi-junction thermopile of the plated (copper-constantan) wire wound type which is temperature compensated in order to get a response that is independent of ambient temperature. The temperature sensed by the detector is nearly linear with the flux density of incident radiation. The instrument is supplied with a pair of removable precision ground and polished concentric hemispheres of Schott optical glass. The inner hemisphere is transparent to a wavelength of 0.28-3.0 μm .

The outer dome can be replaced by Schott glass hemispherical filters which transmit within specified bandwidths. Desiccant is placed in the side of the instrument to absorb humidity inside the glass domes.

OBSERVATIONS AND ANALYSIS TECHNIQUES

Method of Data Archive

A compact, hand-held Radiometer (Sun-photometer and Ozonometer versions of Microtops-II), which utilizes direct solar light observations at discrete wavelengths has been used to characterize aerosols and pre-cursor gases in the Antarctic region. Continuous measurements were made at the Indian station 'Maitri' (70.76°S, 11.74°E, 117 m AMSL) during the southern summer months of December to February. High-resolution solar radiometric observations of aerosol optical depth (AOD) at six wavelengths, covering from UV to NIR (380, 440, 500, 675, 870 and 1020 nm), total column ozone (TCO) and precipitable water content (PWC) have been estimated. The differential optical absorption and scattering (DOAS) method has been followed for the measurement of TCO (300, 305 and 312.5 nm) and PWC (940 and 1020 nm). The data sets were recorded at 10-minute interval, when the variation in zenith angle is faster (and hence rapid changes in air mass) and at 30-minute interval during the intermediate period. For each data set, photometers were operated initially by keeping the cover closed for the optical blocks (consisting of windows, filters etc.). During this period, the instruments stored the background values for all the filters. In the next few seconds, on removing the cover, they collected a set of over 25 observations for each filter. The average value, thus obtained for each filter, was used to compute the spectral variation of columnar AOD, ozone and precipitable water content instantaneously, and several other system parameters like power density, calibration constant, instrument temperature etc. recorded at each wavelength, have been depicted on the display for a quick look, and stored in the memory. Thus, a total of more than 30-35 sets of observations of direct solar radiation have been collected from sun-rise to sun-set on each experimental day.

Data were archived during different sky conditions from December 2004 to March 2005. In view of complexity involved in the data analysis procedures, observations collected during clear-sky conditions only were utilized in the present study. Calibration of both photometers was performed by a transfer of calibration constants from reference instruments which were calibrated by the Langley plot technique at a noise-free high-altitude

site. The AOD, TCO and PWC were evaluated from the data reduction. The analysis techniques have been described in the sections to follow.

Data over the oceanic region also have been collected on-board ship during onward and return journey. Short-term variations in TCO have been studied using data sets that were collected at 10-15 minutes interval on clear-sky days.

An important advantage with this radiometer as compared to many complementary instruments lies in its portability and on-line data acquisition and analysis. This enabled us to obtain simultaneous estimates of aerosol and pre-cursor gaseous optical depths instantaneously. More details about observational scheme, calibration and data retrieval procedures for this radiometer have been published (Devara et al., 2001; Ichoku et al., 2002). In addition, short-wave global radiation fluxes using a wide-band pyranometer have been carried out. By combining pyranometer and sun-photometer observations, direct radiative forcing due to aerosols on clear-sky days has been computed (Maheskumar and Devara, 2004). These extensive data sets, collected during January-February 2005, have been utilized to investigate the aerosol optical, micro-physical and radiative properties, and their interface with simultaneously measured gases such as total column ozone, water vapor, and surface-level meteorological parameters.

DATA RETRIEVAL TECHNIQUES

Retrieval of Aerosol Optical Depth and Size Distribution

The optical depth of the atmosphere can be determined from the Beer-Bouger-Lambert law, expressing attenuation of the direct solar beam in the atmosphere in the form

$$I(\lambda) = I_0(\lambda) [\exp(-\tau_{total}(\lambda) m(\chi))] \quad \dots (1)$$

where $I(\lambda)$ is the monochromatic solar irradiance reaching the instrument detector at wavelength λ , $I_0(\lambda)$ is the irradiance incident at the top of the atmosphere and it can be used to self calibrate the system, m is the optical air mass, which is a function of solar zenith angle, χ [$m = \sec(\chi)$]. From the straight line fitting to the data points of the plot of natural logarithm of radiometer output versus air mass (Langley plot), the atmospheric total optical depth ($-\tau_{total}$) is given by

$$\tau_{total}(\lambda) = \tau_m(\lambda) + \tau_g(\lambda) + \tau_a(\lambda) \quad \dots (2)$$

where $\tau_m(\lambda)$ is the optical depth due to air molecules (Rayleigh scattering); $\tau_g(\lambda)$ is the optical depth due to gas molecular absorption (i.e. due to gases that are expected to contaminate the measurements), which may be useful in determining the columnar content of the atmospheric species or gases such as ozone, precipitable water content and $\tau_a(\lambda)$ is the optical depth due to aerosol particles. $\tau_m(\lambda)$ can be evaluated by knowing the refractive index of air molecules and molecular number density of air at standard atmospheric temperature and pressure. $\tau_g(\lambda)$ can be computed from absorption cross-section of different gas molecules at any wavelength and from known number density of the absorbing gas. $\tau_a(\lambda)$ can be computed by subtracting $\tau_m(\lambda)$ and $\tau_g(\lambda)$ from $\tau_{\text{total}}(\lambda)$. The size distribution of aerosols is obtained by inverting the spectral variation of AOD using the constrained linear inversion scheme (King et al. 1978; King, 1982) with the Fredholm integral as

$$\tau_a(\lambda) = \int_a^b \pi r^2 Q_{\text{ext}}(r, \lambda, m) n_c(r) dr, \quad \dots(3)$$

where Q_{ext} is the aerosol extinction efficiency factor which depends on the aerosol refractive index (m), radius (r) and the wavelength of incident radiation (λ) and $n_c(r)$ is the columnar size distribution function of aerosols (number of aerosols in a vertical column of unit cross section in a radius range dr centered at r and r_a and r_b are respectively the lower and upper radii limits of integration. Since $n_c(r)$ cannot be written analytically, a numerical approach is followed to separate $n_c(r)$ into two parts as $n_c(r) = h(r) \cdot f(r)$, where $h(r)$ is rapidly varying function with r and $f(r)$ is slowly varying. Hence the above equation becomes

$$\tau_a(\lambda) = \sum_{j=1}^q \int_{r_j}^{r_{j+1}} \pi r^2 Q_{\text{ext}}(r, \lambda, m) h(r) \cdot f(r) dr, \quad \dots(4)$$

In the above equation, the quadrature error will be less if $f(r)$ is assumed as constant. In that case, a system of linear equations results, which may be written as

$$\tau_a(\lambda) = A f(r) + \varepsilon \quad \dots(5)$$

where

$$A = \int \pi r^2 Q_{\text{ext}}(r, \lambda, m) h(r) dr$$

and ε is an error which arises due to deviation between the measured τ_a and theoretical $\tau_a = \sum A_{ij} f_i$.

Retrieval of Total Column Ozone and Precipitable Water Content

The measurement technique followed for monitoring total column ozone (TCO) and precipitable water content (PWC) in the present experiment utilizes the principle of differential optical absorption at two nearby wavelengths of Sun's UV and near IR radiation, respectively. In the case of ozone, the measurement of solar irradiance in the UV region (300 and 305 nm) is basically used to calculate the TCO. The measurement at additional third wavelength (312.5 nm) enables correction for particulate scattering and stray light.

The columnar precipitable water content is determined based on the measurements of solar irradiance at 940 nm (H_2O absorption peak) and at 1020 nm (nil or less absorption) by water vapor. The AOD at 1020 nm is also calculated based on the extra-terrestrial radiation at this wavelength, corrected for Sun-Earth-distance, and the ground-level measurements of radiation at 1020 nm. The optical depth at NIR in conjunction with those from the sun-photometer at UV and V regions are utilized to retrieve columnar aerosol size distribution (ASD) by applying the constrained linear inversion method.

Estimation of Aerosol Radiative Forcing

Aerosol radiative forcing is computed using the differential method as explained by Conant (2000). This method assumes that changes in the range of 0.3 - 3 μm solar flux are forced by changes in aerosol optical depth, and is not sensitive to small calibration uncertainties. In this method, reference flux is chosen on the basis of following assumptions.

- 1) Observed flux (A_s) is available for both morning and afternoon at each zenith angle (θ).
- 2) AOD (τ) is mostly invariant over all values of zenith angle (θ)
- 3) It has the lowest optical depth in the sample.

From the daily mean AOD and solar flux values, for all clear-sky days in each month, the day of minimum AOD and corresponding flux is

taken as reference day. The deviations between this reference AOD and flux values from each diurnal mean AOD, net AOD and net flux are calculated.

$$\langle \Delta\tau \rangle (\text{diff}) = \langle \tau \rangle - \langle \tau \rangle (\text{ref day})$$

$$\langle \Delta A_s \rangle (\text{diff}) = \langle A_s \rangle - \langle A_s \rangle (\text{ref day})$$

In order to avoid the influence of air mass, these deviations thus obtained AODs and fluxes are normalized with air mass.

$$\langle \Delta\tau \rangle (\text{diff}) / \text{Air mass} = \langle \Delta\tau \rangle (\text{Normal})$$

$$\langle \Delta A_s \rangle (\text{diff}) / \text{Air mass} = \langle \Delta A_s \rangle (\text{Normal})$$

The graph between normalized AOD (abscissa) and normalized flux (ordinate), the slope gives 'Forcing Efficiency'. The product of forcing efficiency and monthly mean AOD gives 'Radiative Forcing' for that month.

DISCUSSION OF RESULTS

Spectral Characteristics of Aerosols

Wavelength Dependence of Aerosol Optical Depth (AOD)

Figure 3 (a & b) depicts the spectral distribution of AOD observed on two typical clear-sky days. These plots reveal that AOD initially decreased from 340 to 440 nm wavelength and then slightly increased with increasing wavelength. This implies that loading of larger particles dominated

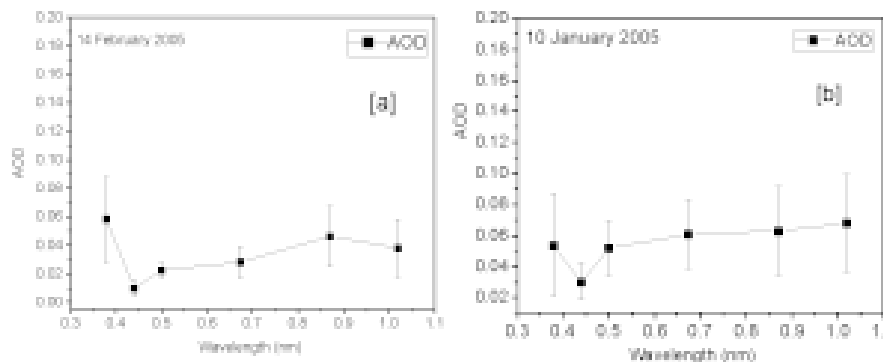


Fig. 3 : Wavelength dependence of AOD for two typical clear-sky days.
The vertical bars indicate error in the measurement

that of the sub-micron particles in the atmosphere. This is also consistent with the observed Angstrom exponent (Alpha) values (indicator of aerosol size distribution), which are discussed in the next Section. This could be due to influx of marine and continent (natural) aerosols that prevails over the experiment site through transport phenomenon.

Daily Mean Spectral Distribution of AOD

The day-to-day variations in AOD at three characteristic wavelengths of 340, 500 and 1020 nm, representing fine, sub-micron and larger aerosol particles, together with Angstrom exponent (Alpha) observed during clear-sky conditions in the months of January and February 2005 are shown plotted in **Figure 4**. The daily mean AOD was found to be 0.042 with an average Angstrom exponent of 0.24, revealing the abundance of coarse-mode particles. It is interesting to note from the above figure that January AODs were higher as compared to those of February with smaller values of Alpha indicating dominance of larger particles (coarse-mode) in January and larger values of Alpha revealing the dominance of smaller particles (fine-mode) in February.

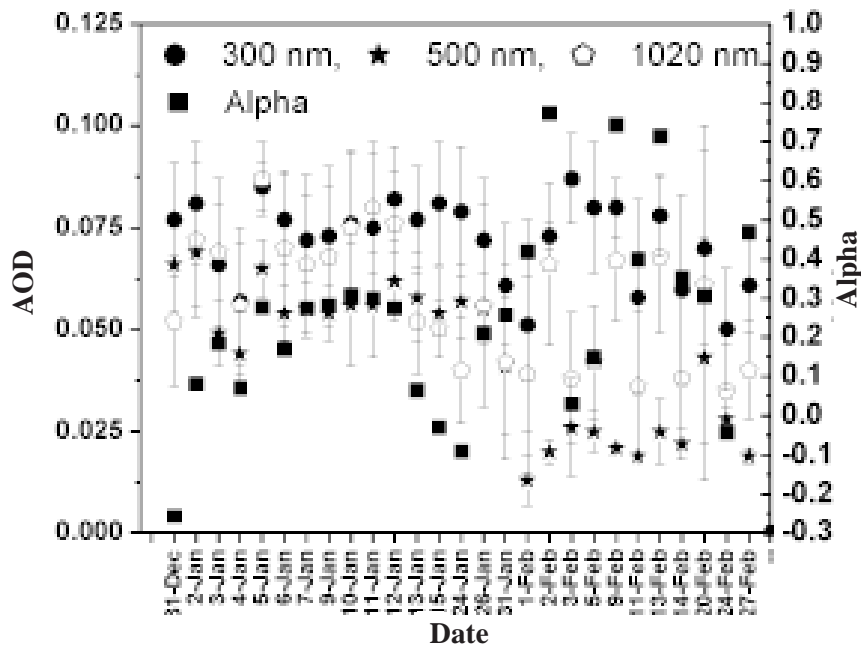


Fig. 4 : Day-to-day mean variation in AOD and Alpha over Maitri. The vertical bars denote standard error in the estimation

Aerosol Size Distribution (ASD)

The aerosol size spectra, retrieved from the wavelength dependence of aerosol optical depth, have been obtained by following the constrained linear inversion method. The aerosol size distributions, computed on a few typical clear-sky days in January and February months are shown in **Figure 5**. These distributions, on an average, exhibit bi-modal and tri-modal distributions during the study period. As evidenced from the figure, the size distributions exhibit almost equal dominance in accumulation and coarse modes, and reveal distinct difference in both the months. In February, besides dominance of coarse-mode particles, tri-modal distribution (each mode representing different sources & size of particles) with a primary

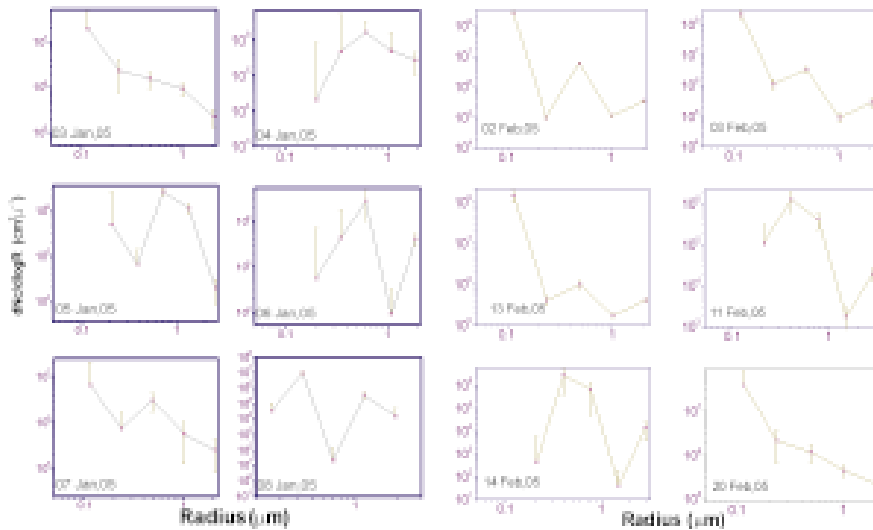


Fig. 5 : Aerosol size distribution observed on some typical days during the study period

mode at 0.1 – 0.6 micrometer and secondary mode at 0.6 - 1.0 micrometer, and third mode of particle size at 1.0 - 1.2 micrometer (coarse mode) could be noted. The formation of primary mode particles is considered to be due to gas-to-particle conversion and photochemical reaction processes while that of coarse-mode particles is ascribed to the water bubble bursting (white caps) process over oceanic, and wind-blown from continental regions.

Variations in Aerosol and Pre-cursor Gas Characteristics

Temporal Variations in Aerosol Optical Depth (AOD)

Figure 6 portrays time evolution of AOD at discrete wavelength of near UV, Visible and near IR viz. 340, 440, 500, 675, 870 & 1020 nm, representing fine, sub-micron and larger aerosol particles observed during clear-sky conditions in January and February 2005. The two features that can be seen commonly at all wavelengths on both days are (i) greater AODs during forenoon hours, which can be explained on the basis of advection

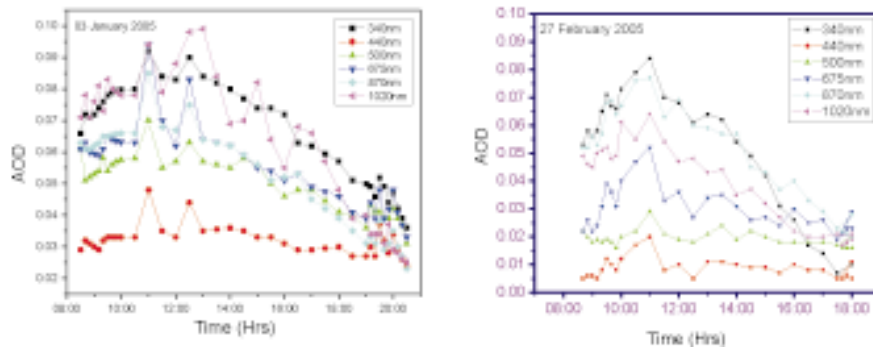


Fig. 6 : Diurnal variation of AOD on two typical days

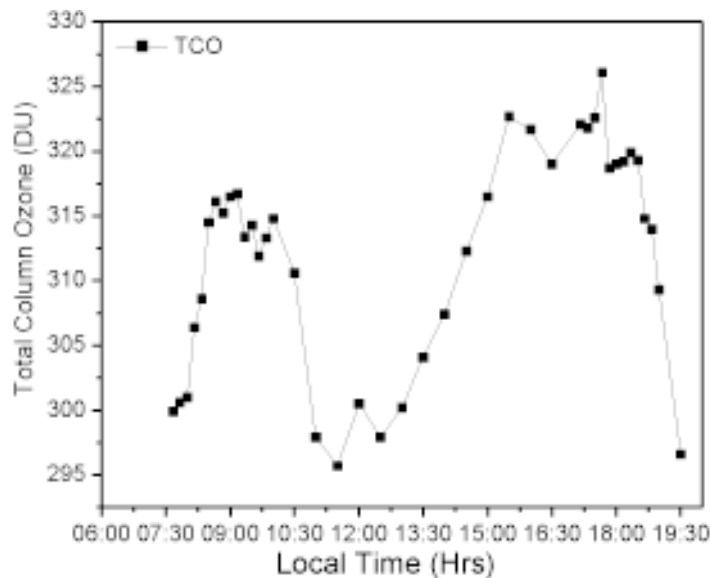


Fig. 7 : Temporal variation of Total column ozone (TCO) on December 29, 2004

of pollutants from surrounding (for example, toilet firing, power generator smoke etc.), and (ii) increase in AOD during forenoon hours and decreases during afternoon hours at all wavelengths. The time variation of AOD_{500} shows very low aerosol optical depth (ranging between 0.26 and 0.77 with an average value of 0.24) with significant variations throughout the observation period at the experimental site.

Temporal Variations in Total Column Ozone (TCO)

In order to illustrate the nature of diurnal variation of ozone at Antarctica, high resolution data collected on a typical clear-sky day have been plotted in **Figure 8**. The diurnal variation in ozone showed two maxima during day time, one in the forenoon and the other in the late afternoon hours. There is a distinct minimum around 1200 hrs local time. The primary peak is mostly due to either gradual lifting from ground-level or trapping of gases that are evolved due to anthropogenic activities. The secondary peak, around afternoon hours, is mainly due to photochemical reactions. Thereafter the values were found to decrease towards larger zenith angle. Figure 8 shows the latitudinal variation of the total column ozone, which showed gradual increase in ozone with increasing latitude in Southern Hemisphere (252 DU around 38° S to about 312 DU at 70° S) and the decrease in total ozone from morning till noontime over the high-latitude oceanic region also.

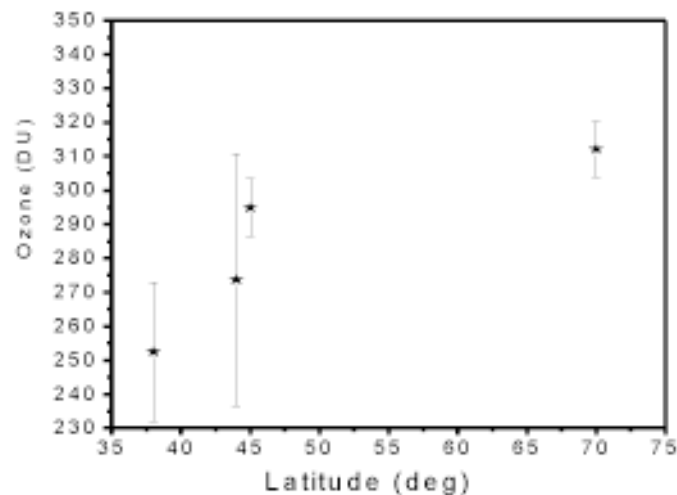


Fig. 8 : Latitudinal variation of TCO during the study period

Temporal variations of Total Column Precipitable Water Content

The day time diurnal variations of PWC during different sky conditions were studied during observation period. Such variations observed on a typical day are shown in **Figure 9**. The value of PWC was found to be in the range of 0.23 to 0.36 cm, which is very low compared to other continental regions. The PWC showed an increasing trend from morning to evening and attained the maximum in the evening hours on almost all the observation days during both months. This variation may be due to surface level wind speed which picked up at evening time. It is observed that these values were initially lower and thereafter it increased toward evening hours while there values were higher even from the beginning of the day.

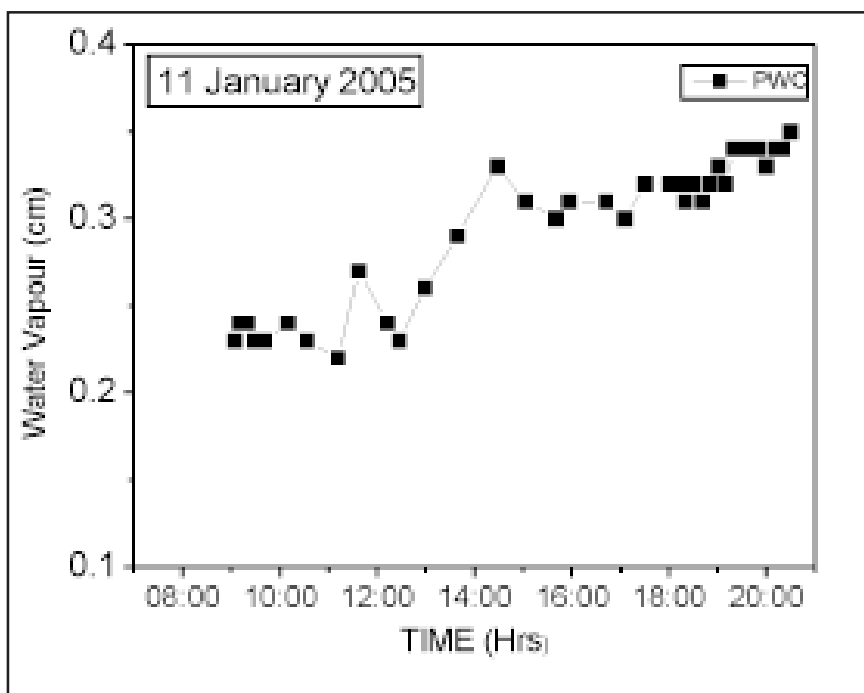


Fig. 9 : Temporal variation of PWC on January 11, 2005

Day-to-day variation in TCO & PWC

The day-to-day variation in total column ozone (TCO) and water content (PWC) were found to exhibit an inverse relationship on particular days associated with low temperature (**Figure 10**). In the month of January (mid-summer period), the ozone concentration showed high (~255 to 280

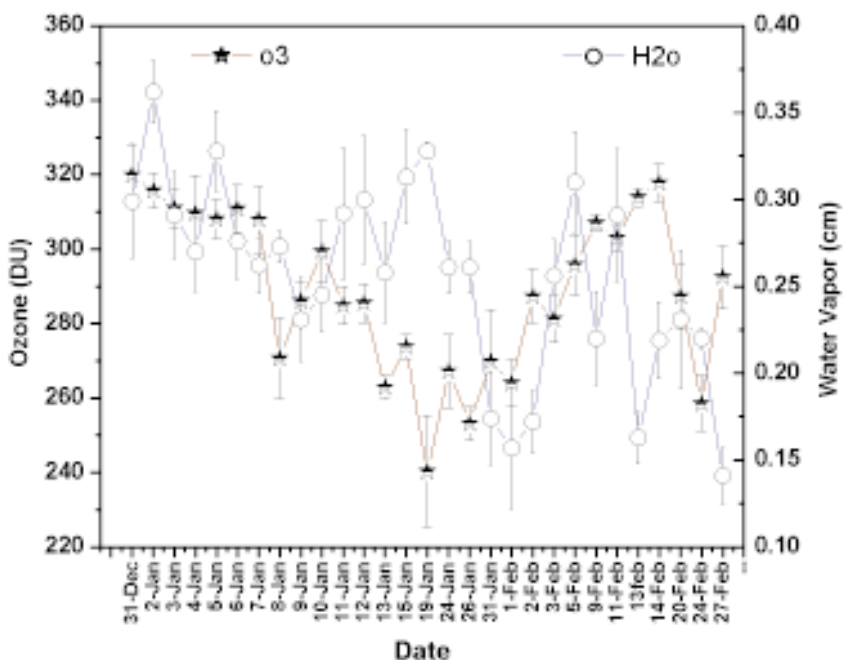


Fig. 10: Daily mean variations in TCO and PWC (H_2O) over Maitri. The vertical bars denote standard error in the estimation

DU) and low values of PWC (0.36 to 0.14 cm), which could be due to strong convective activity and associated photochemical activity. As we approach towards winter period i.e. in February, the ozone concentration decreased (between 220 and 310 DU) with increase in the PWC from 0.14 to 0.33 cm. This could be attributed to the relationship resembling that of heterogeneous chemical processes wherein aerosols act as catalysts in the ozone destruction mechanisms, resulting in reduction in ozone amount. During the total observation period, TCO and PWC were found to vary from 240 DU to 320 DU with an average value of 289 DU, and from 0.14 to 0.36 cm with average value of 0.26 cm, respectively.

Comparison between Ozone measurements by Microtops II and TOMS

Variability in ozone on daily scale during the period of observation was less than 4% over the Antarctic region. Day-to-day variation in total column ozone over the Indian Antarctic station is shown in Figure 10 by computing daily means for the entire period of Day number 1 in the figure denotes January 01, 2005. The figure also shows the daily observation of

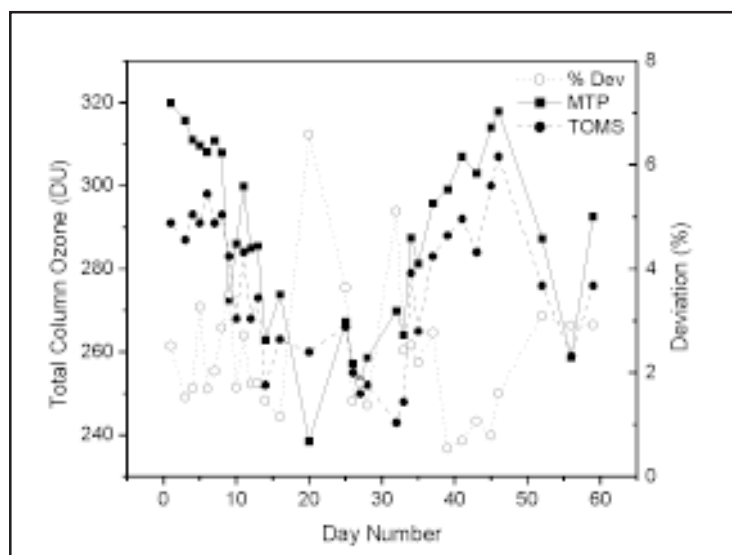


Fig. 11 : Comparison between ozone contents from TOMS and Ozonometer observations

total ozone from TOMS satellite data **Fig. 11**. It can be seen from the figure that there is a good agreement between the two observations while the surface measurements slightly overestimating, but within 6% deviation. It is interesting to note that both ozonometer and TOMS have recorded a substantial decrease of ozone, by almost 50 DU, during the second half of January.

Radiative Forcing

In the present study, the radiative forcing was calculated at 500 nm wavelength combining the AOD data from the MICROTOPS II sun photometer and concurrent radiative flux measured by the pyranometer. **Figure 12** shows the diurnal variation in radiation fluxes observed on some typical days, which revealed bell-shape with maximum flux around local noon and minimum around early morning and late evening hours. The decrease in flux in the presence of clouds may be seen very clearly from the figure. Such observations will be useful to discriminate the clear-sky AOD from cloudy-sky AOD.

These variations in radiative forcing **Fig. 13** reveal that the forcing swings between positive (warming) and negative (cooling) during January, while it is negative during February, which is considered to be due to influence of local meteorology and also due to long-range transport of aerosol loading.

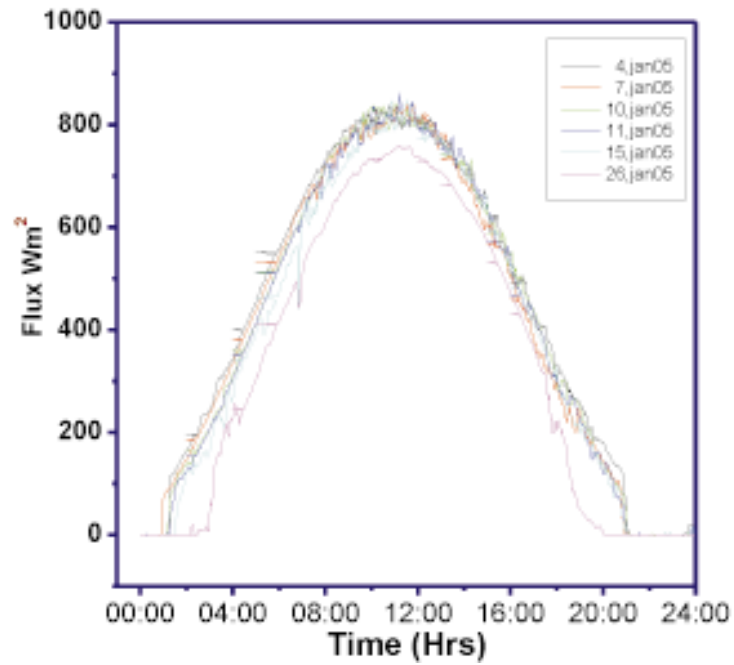


Fig. 12 : Diurnal variation in radiant flux on different experimental days

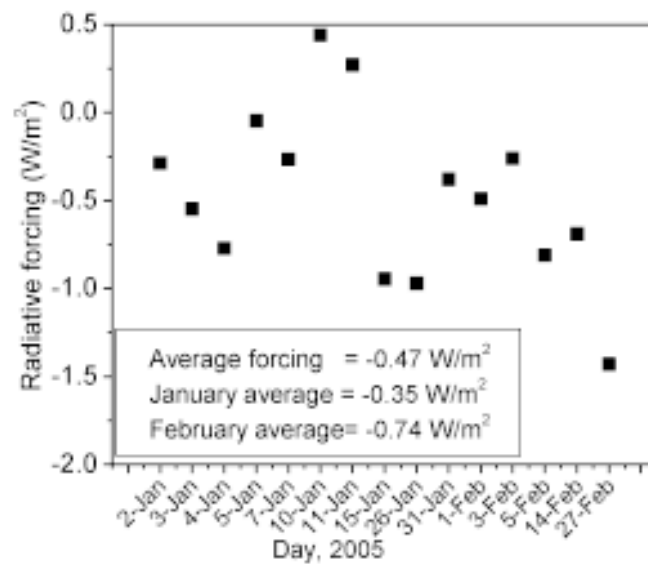


Fig. 13 : Variations in daily average radiative forcing

The forcing values were found to vary between -1.44 W/m^2 and 0.44 W/m^2 with an average value of -0.47 W/m^2 during the period of study. These values were found to be consistent with reported values in the literature, and have strong bearing on changes in surface albedo and Sun-Earth geometry during the experimental period.

SUMMARY AND CONCLUSIONS

Aerosols and pre-cursor gases are of considerable interest in atmospheric sciences, mainly due to their potential of changing the radiative transfer of solar radiation. As Antarctica is the remote polar region characterized by the highest surface albedo and one of the less illuminated by solar radiation for a major time period during the year, detailed studies relating to characterization and impact of these constituents are highly essential. Moreover, the Antarctic continent can be expected to provide reference levels for all environmental and pollution studies due to its remoteness and restricted human activities. Aerosols are currently the largest source of uncertainty for characterizing the radiative forcing of climate (Schwartz et al., 1990). To evaluate the influence of aerosols, we need to quantitatively attribute aerosol forcing to aerosol type (natural and anthropogenic) for highly diverse conditions. (Rathke et al., 2002), The present experimental study, carried out at Maitri, as part of the 24th IAE, revealed the following :

- ◆ The mean AOD at 500 nm was found to vary from 0.013 to 0.069 with an average value of 0.042. The Angstrom exponent (Alpha) which is an indicator of aerosol size distribution, was found to vary between 0.26 and 0.77 with an average value of 0.24.
- ◆ The aerosol size distribution showed distinct difference between January and February months. In February, coarse-mode particles dominated, tri-modal distribution (each mode representing different sources and sizes of particles) with a primary mode at 0.1 – 0.6 micrometer and secondary mode at 0.6 to 1.0 micrometer (accumulation-mode) and the third mode of particle size at 1.0 to 1.2 micrometer (coarse-mode).
- ◆ The TCO and PWC were found to vary from 240 DU to 320 DU with an average value of 289 DU, and from 0.14 to 0.36 cm with an average value of 0.26 cm, respectively.
- ◆ Day-to-day variation in total column ozone and water vapour exhibited inverse relationship on certain days associated with low temperature,

which revealed heterogeneous chemical processes leading to ozone destruction.

- ◆ Diurnal variation in radiation flux showed bell-shape with maximum flux around local noon and minima around early morning and late evening. The January fluxes were found to be dropped by about 20 % in February.
- ◆ Estimated aerosol radiative forcing showed cooling at the surface, with a value varying between -1.44 W/m^2 and 0.44 W/m^2 with an average value of -0.47 W/m^2 during the period of study.
- ◆ Total column ozone showed a gradual increase with increasing latitude in Southern Hemisphere (252 DU around 380° S to about 312 DU at 70° S).
- ◆ Both ozonometer and TOMS were found to record a substantial reduction in ozone, by almost 50 DU, during the second half of January, and good agreement between the TOMS (satellite observation) with surface observation (Microtops-II) within 6% deviation.
- ◆ Temporal variation in ozone showed two maxima during day time, one in the forenoon and the other in the late afternoon hours with a distinct minimum around 1200 hrs local time.

ACKNOWLEDGEMENTS

This work was supported jointly by the IITM, Pune and NCAOR, Goa. The authors are thankful to NCAOR for providing excellent infrastructure facilities during the period 24th IAE. Thanks are also due to all Members of the IITM Lidar and Radiometric Group, particularly to P. Ernest Raj and K.K. Dani.

REFERENCES

1. Conant, W.C., 2000: An observational approach for determining aerosol surface radiative forcing: Results from the first phase of INDOEX, *J. Geophys. Res.*, **105**, (D12), 15347-15360.
2. Devara, P.C.S., R.S. Mahes Kumar, P. Ernest Raj, K.K. Dani and S.M. Sonbawne, 2001: Some features of aerosol optical depth, ozone and precipitable water content observed over land during the INDOEX-IFP99., *Meteorologische Zeitschrift*, **10**, 901-908.
3. Gadhavi, H. and A. Jayaraman, 2003: Aerosol characteristics and aerosol radiative forcing over Maitri-Antarctica, *Current Science.*, **80**, 296-304.

4. Ichoku, C., L. Levy, Y.J. Kaufman, L.A. Remer, Li. Rong-Rong, V.J. Martins, B.N. Holben, N. Abuhassan, I. Slutsker, T.F. Eck and C. Pietras, 2002: Analysis of the performance characteristics of the five-channel Microtops-II sun-photometer for measuring aerosol optical thickness and precipitable water vapor, *J. Geophys. Res.*, **107**, D13, 10.1029/2001JD001302.
5. IPCC, 1995, Climate Change 1995: The Science of climate change, [Houghton, J.T. et al., (eds.)]. Cambridge Univ. Press, 572. 15.
6. Jain, S.L., B.C. Arya, S. Ghude, A. Kumar and P.C. Pandey, 2004: Measurement of green-house gases and ozone at Maitri, Antarctica, *Proc. XXVIII SCAR Open Science Conference*, Brochure 2004.
7. King, M.D., D.M. Byrne, B.M. Herman, and J.A. Reagan, 1978: Aerosol size distribution obtained by inversion of spectral optical depth measurements, *J. Atmos. Sci.*, **35**, 2153-2167.
8. King, M.D., 1982: Sensitivity of Constrained linear inversions to the selection of the Legendrian multiplier, *J. Atmos. Sci.*, **39**, 1356-1369.
9. Maheskumar, R.S. and P.C.S. Devara, 2004: Observational estimation of direct radiative forcing by atmospheric aerosols, Proc. International Conference on 'Aerosols, Clouds and Indian Monsoon', IIT, Kanpur, India, November 15-17, 2004, *IASTA Bulletin*, **16**, 30-33.
10. Panneerselvam, C., K. Jeeva, K. U. Nair, S. Gurubaran., R. Rajaram., Ajay Dhar and G. Rajaram, 2004: Observation of Atmospheric Maxwell Current at Indian Antarctica Station, Maitri. *19th Indian Antarctica Expedition, Scientific Report*, No.17, pp 99-105.
11. Penner, J.E , M.O. Andreae, L. Annegarn, J. Barrie, G. Feichter., D. Hegg, A. Jayaraman, R. Leaitch, D. Murphy, J. Nagana, and G. Pitari, 2001: Aerosols , their Direct and indirect effects in climate change: IPCC Report , Cambridge University Press, 289-348.
12. Rajaram, G., and B.M. Reddy, 1993: Atmospheric Research from Antarctica – The Indian Contribution, DST/ CSIR Publ., 104pp.
13. Ramanathan, V., P.J. Crutzen, J.T. Kiehl and D. Rosenfeld, 2001: Atmosphere aerosol Climate and the hydrological cycle, *Science*, **294**, 2119-2124.
14. Rathke, C., 2002: Properties of Coastal Antarctica aerosols from combined FTIR Spectrometer and Sun-photometer measurements, *Geophys. Res. Lett.*, **29**, 2123-2131.
15. Russell, P. B., J. M. Livingston , P. Hignett., S. Kinney., J. Wong., And Hobbs P. V.,1999: Aerosol – induced radiative flux changes off the united state mid- Atlantic coast; comparison of values calculated from sun photometer and in situ data with those measured by airborne pyranometer, *J. Geophys. Res.*, **104**, 2289-2307.
16. Schwartz, S.E., and Co-authors, 1990: Uncertainty in climate change caused by aerosols, *Science*, **272**, 1121-1122.
17. WMO (World Meteorological Organization), *Scientific Assessment of Ozone Depletion: 2003*, Global Ozone Research and Monitoring Project – Report No. 47, 498pp.